

PAPER • OPEN ACCESS

Particulate Matter Load Estimation and Distribution Characteristics of Diesel Particulate Filter

To cite this article: Jiguang Wang *et al* 2023 *J. Phys.: Conf. Ser.* **2528** 012019

View the [article online](#) for updates and enhancements.

You may also like

- [Review of black carbon emission factors from different anthropogenic sources](#)
Topi Rönkkö, Sanna Saarikoski, Niina Kuittinen *et al.*
- [Delay effects of the interactions between neutrons emitted during plasma experiments performed on the DPF-1000 U facility and construction materials](#)
Kamil Szewczak and Sawomir Jednorog
- [Effect of the amount of trapped particulate matter on diesel particulate filter regeneration performance using non-thermal plasma assisted by exhaust waste heat](#)
Yunxi SHI, , Yixi CAI *et al.*



244th ECS Meeting

Gothenburg, Sweden • Oct 8 – 12, 2023

Register and join us in
advancing science!

Learn More & Register Now!



Particulate Matter Load Estimation and Distribution Characteristics of Diesel Particulate Filter

Jiguang Wang^{a,b}, Feng Xu^{a,b*}, Li Wang^{b*}, Xudong Chen^{a,b}, Qiuling Chen^a, Fei Han^a, Youxian Huang^a, Xuan Li^a, Qingyun Xu^a, Yu Ge^a, Wangwen Gu^a, Xinghai Dai^a

^aCARARC Automotive Test Center (Kunming) Co., Ltd, No.16 Donghuan Road, Kunming, 651701, China

^bChina Automotive Technology and Research Center Co. Ltd, No.68 Xianfeng East Road, Dongli District, Tianjin, 300300, China

Corresponding author: xufeng@catarc.ac.cn, wangli@catarc.ac.cn

Abstract: This paper focuses on the offline electric heating regeneration technology of DPF (Diesel Particulate Filter). Based on the actual operating conditions of the airport passenger elevator, the pressure drop changes before and after the offline regeneration of DPF, the passive regeneration process during the vehicle operation, and the capture efficiency of PM and PN after the offline regeneration of DPF are studied. The DPF pressure drop increases with the operation time because of the extremely low efficiency of passive regeneration before offline regeneration, and the initial pressure drop after regeneration is slightly higher than that of the fresh carrier due to the existence of ash. When the exhaust temperature reaches 420°C, the DPF passive regeneration rate is higher than the capture rate, and the DPF pressure drop drops rapidly when the passenger elevator continues to run. The mass fraction of fine particulate matter is more than 0.02μm in the cold start stage, while the mass fraction of fine particulate matter is more than 0.02μm in the hot start stage.

1. Introduction

Diesel Particulate Filter (DPF) is currently recognized as the most effective technique for reducing particulate matter emissions from diesel engines^[1] and has been widely used in diesel vehicles and non-road diesel machinery particulate matter emissions control^[2-3].

The Civil Aviation Administration of China proposed a "Three-Year Action Plan for Winning the Blue Sky Defense War" that the in-use gasoline and diesel vehicles belonging to China III and below emission standards should achieve 100% exhaust gas retrofit^[4]. As a special workplace, the airport flight control area has high requirements for the safety of vehicles operating around the aircraft. At the same time, the vehicles have operating characteristics such as low-speed operation, high power, long operation time, and low exhaust temperature during operation, which brings great difficulty to the vehicle exhaust control and retrofit in the airport flight control area. Considering the impact on the aircraft at the airport, Beijing Capital Airport requires the use of passive regenerative DPF devices that do not allow dangerous substances, such as open flames, to appear in the emission control. However, in the actual emission control, due to the actual situation, such as low exhaust temperature and poor emission, it is difficult for the traditional passive regeneration technology to achieve regeneration^[5-6],



resulting in a sharp shortening of the period of DPF regular maintenance and cleaning, and an increase in the frequency, which seriously affects the treatment^[7-8].

To effectively solve the technical scheme of exhaust emission control of vehicles in the airport flight control area under special operating conditions, this paper selects a diesel passenger elevator car as the test vehicle at Tianjin International Airport, and adopts the new "DOC+DPF+off-line electric heating technology^[9]" to carry out emission control retrofit and demonstrations, research and analyze the characteristics of the DPF capture and regeneration process cycle, frequency, and other characteristics of the test vehicle in actual operation, as well as the impact on the emission reduction effect of PN and PM concentration.

2. Test devise and program

2.1. Test vehicle

A TK-KT58 diesel aircraft passenger elevator vehicle (produced in May 2015, curb weight 8500kg) in Tianjin International Airport, which has reached the China III emission standard, was selected to demonstrate particulate emission control. There is no pollution control device in the original exhaust system of the test vehicle. Only a muffler is installed. In the test process, the offline electric heating technology device was mainly used to replace the muffler in the original chassis emission control system for emission retrofit and upgrading, as shown in Figure 1.



Fig.1 Test vehicle and exhaust system after retrofit

2.2. "DOC+DPF+off-line electric heating technology" device

The offline electric heating technology device installed on the vehicle is mainly composed of the diesel oxidation catalyst (DOC) + DPF and an electric heating device system, as shown in Figure 2. There is a connection interface for installing the electric heating device system at the inlet end of the DPF. When the vehicle and DPF are in the daily operation process, the electric heating device system is not placed in the inlet end of the DPF, and its connection interface is fixed and closed with a cover plate, as shown in Figure 3. When regeneration is required, use a wrench and other tools to open the connection interface and then install the electric heating. The device system is connected and fixed with the DPF body through the clamp, and then the external 380V electric heating and maintenance control box system is used to supply power to the electric heating device system for DPF regeneration.

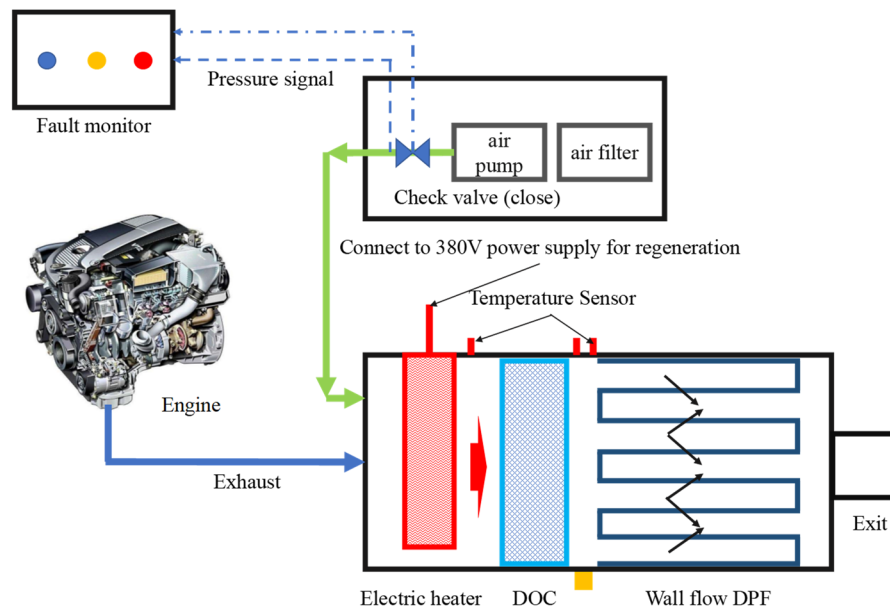


Fig. 2 Offline electric heating DPF system structure



Fig.3 Offline electric heating and maintenance equipment

The body of the offline electric heating device system is a cylindrical structure. When the external 380V power supply is activated, the electric heating device system will automatically match and control the heat and air volume according to the command of the control module and at the same time, cooperate with the catalyst to make the passive regeneration of the filter faster^[16]. After the regeneration is completed, the electric heating device system is automatically powered off, and the vehicle can continue to work after it is removed. When the machine is working normally, passive regeneration is started, and the electric heating device system does not participate in the regeneration process. When the exhaust gas temperature reaches the regeneration temperature, the catalytic regeneration can be continuously completed. At the same time, the electric heating maintenance control box and the mechanical electric heating system have the function of current overload protection. When the current is overloaded or short-circuited, the whole system will be automatically powered off.

The offline electric heating maintenance control box must be installed and fixed in a dry place away from the fire source, providing a 380V three-phase five-wire power supply. The maintenance process operation should be strictly operated by the specifications and carried out in a place that meets the operating conditions.

2.3. Data collection method

In this paper, remote monitoring and on-site emission test methods are used to study the capture and regeneration performance of DPF and the emission characteristics of PM in actual operation, collect the relevant data of vehicles and DPF devices in actual operation in real-time and transmit by GPRS^[17] to the monitoring platform for big data statistical analysis. The data mainly includes vehicle speed, geographic location, exhaust temperature (°C), and DPF pressure drop (kPa) between the inlet and outlet of DPF. The transmission frequency is 1Hz; the on-site emission test mainly uses ELPI (Electrical Low-Pressure Impactor) device to test PM and PN concentration before and after DPF on the passenger elevator car. During the test, to ensure the same test conditions, a special recorder was used to automatically record the speed data (1Hz), and the same driving conditions were reproduced in the test.

ELPI can measure the emission of exhaust particles in real time^[18] and can record the transient number concentration and mass concentration of particles on different diameter segments in 12 grades. The diameter reflects the distribution trend of quantity and quality on different particle size segments through post-processing.

2.4. Remote monitoring data processing method

In the DPF emission remote monitoring big data, due to poor network signal, DPF remote monitoring system failure, and other reasons, the data of some parameter items are missing and abnormal. Carry out the necessary screening, cleaning, and processing^[19]. Data cleaning is mainly to screen and process the collected data, and the key is to determine the "outliers." The data processing method in this research mainly adopts the combination of threshold judgment and interpolation calculation to process the data.

(1) Missing values, mainly the parameters of vehicle speed, exhaust temperature, and exhaust pressure drop, are null;

(2) Outliers are mainly screened by the threshold judgment method. Any combination that meets any of the following conditions is considered an outlier and should be deleted.

①The speed of the test vehicle is less than 0km/h or greater than 60km/h;

②Exhaust temperature is less than 0°C or greater than 1000°C (reference value provided by DPF manufacturer);

③ The exhaust back pressure is less than 0kPa or more than 40kPa (reference value provided by DPF manufacturer);

(3) After missing values and deleted outliers, the average interpolation method is used to fit the parameter data, namely:

$$Diff_t = (D_t + D_{t-1}) / 2 \quad (1)$$

Where $Diff_t$ —fitted value

D_t —The value of a parameter item in the collection of the t^{th} data

D_{t-1} —The value of the acquisition parameter item of the $t-1^{\text{th}}$ data

a —Acceleration value, m/s^2 .

3. DPF pressure drop prediction model

The wall-flow DPF used in this paper is closed in space and has good symmetry characteristics^[10]. Therefore, to simplify the analysis process, a set of inlet and outlet channels are used as the research object for mathematical modeling.

$$\Delta P_{\text{model}} = \frac{\mu Q_v}{2V_{\text{trap}}} (\alpha + \omega_s)^2 \times \left[\frac{\omega_s}{K_0} + \frac{1}{2K_p} \ln\left(\frac{\alpha}{\alpha - 2\omega}\right) + \frac{4FL^2}{3} \left(\frac{1}{(\alpha - 2\omega)^4} + \frac{1}{\alpha^4} \right) \right] + \frac{32\rho_s \xi Q_v^2 (\alpha + \omega_s)^4}{\pi^2 D^4 \alpha^4} \quad (2)$$

Where ΔP_{model} is the pressure drop value of the DPF model; Q_v is the exhaust volume flow; μ is the exhaust dynamic viscosity, which is related to temperature; V_{trap} is the DPF filter volume; α is the filter pore density; ω_s is the filter wall thickness; K_0 is the permeability avoided by the filter body in the fresh state, usually obtained by experiments or given by the manufacturer; K_p is the permeability of the particle layer; ω is the thickness of the particle layer; ρ_s is the exhaust density; F is the friction factor,

generally taken as $F = 28.454$; L is the pore length of the filter body; D is the diameter of the filter body; ξ is the sum of the local loss coefficients at the entrance and exit of the filter body, generally taking $\xi=0.82^{[11-12]}$.

It can be seen that the DPF pressure drop is related to the exhaust volume flow Q_v , dynamic viscosity u , carrier geometric parameters, carrier avoidance permeability, soot permeability, and other parameters related to engine operating conditions^[13]. For a DPF carrier with fixed physical parameters and under steady-state engine conditions, before the particle layer is formed, ω soot is 0, and the DPF pressure drop ΔP is only related to the wall permeability $K_{wall}^{[14]}$. With the loading of particles, a particle layer will gradually form on the wall of the carrier inlet channel. At this time, the DPF pressure drop is also related to the thickness ω soot of the soot layer and the permeability of $K_{soot}^{[15]}$.

It can be seen from Equation (2) that the DPF pressure drop and exhaust flow have a quadratic relationship. For a DPF with a certain filter parameter, Equation (2) can be simplified as Equation (3):

$$\Delta P_{model} = A Q_v + B \rho_s Q_v^2 \quad (3)$$

Exhaust density as equation (4)

$$\rho_s = \frac{(T_{DPF} + 273.15) \times 287.15}{(T_{DPF} + 101.15) \times 1000} \quad (4)$$

Where T_{DPF} is the bed temperature of the DPF; P_{DPF} is the pressure drop at the front and rear ends of the DPF.

4. Data processing and result analysis

4.1. Test vehicle operating conditions and exhaust temperature characteristics

According to the relevant regulations of the airport, the speed limit of vehicles in the airport is 50 km/h, and long-term low-speed driving is likely to cause vehicle emissions to fail to meet the standard^[20]. The operating trajectory and operation characteristics of the aircraft passenger elevator car in the airport are relatively fixed. According to the landing situation of the airport flight, the passenger elevator car will be driven from the parking lot to the designated location on the apron and then stop. The actual running trajectory of the test passenger elevator car was obtained through the GPS signal of the remote monitoring system in the DPF system, and the operating characteristics, running speed, and exhaust temperature of the 15 consecutive days was statistically analyzed.

To facilitate the analysis of vehicle speed and exhaust temperature, the author divided the vehicle speed and temperature range, as shown in Table 1.

Figure 4 shows the statistical distribution of the operating speed and DPF inlet temperature during the operation of the test passenger elevator car. It can be seen that due to the actual characteristics of the airport passenger elevator car, mainly operating when passengers get on and off the plane, it is in an idle state for a long time, accounting for about the total 83% of the working time, while the vehicle speed is maintained at 5~20km/h during operation, accounting for about 14.4% of the total working time. In terms of exhaust temperature, long-term idling and low-speed operation lead to low exhaust temperature of passenger elevators. The operating time below 250°C accounts for 90% of the total operating time, and the operating time between 250°C and 400°C accounts for 10%. It is difficult for the ladder car to be regenerated by passive regeneration technology in actual operation.

Table 1. Speed and temperature range

No	Speed (km/h)	Exhaust temperature T (°C)
A0	$0 < V \leq 5$	$0 < T \leq 50$
A1	$5 < V \leq 10$	$50 < T \leq 100$
A2	$10 < V \leq 15$	$100 < T \leq 150$
...

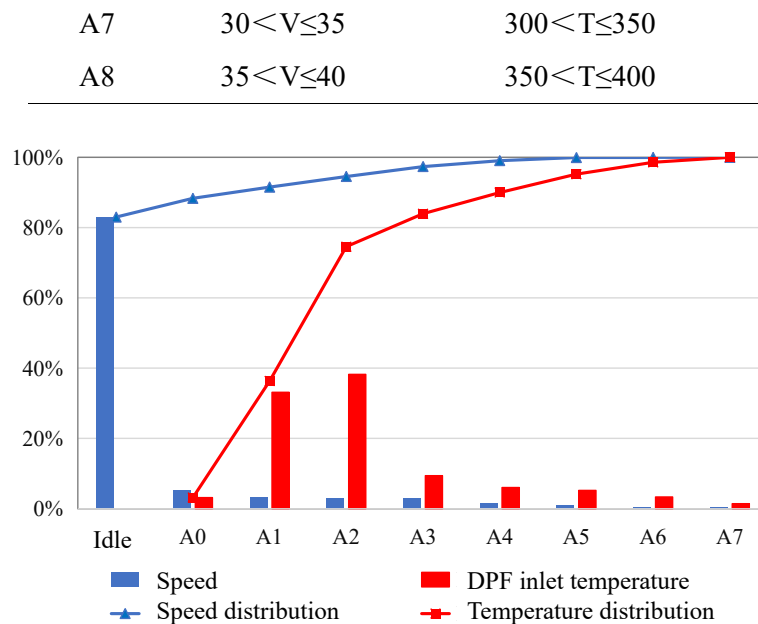


Fig. 4 Statistical distribution of test vehicle running speed and DPF inlet temperature

4.2. DPF loading and regeneration characteristics in actual operation

The degree of loading and regeneration of the DPF device is mainly reflected by the differential pressure sensor signal and the temperature signal. Through the remote monitoring platform and the ΔP_{model} model, the actual and theoretical pressure differences between the front and rear ends of the DPF are obtained, respectively. This paper continuously collects the actual operation data of DPF for two months, from December 11, 2019 to February 9, 2020. To study the characteristics of DPF loading and regeneration cycle and other characteristics, during the test period, Tianjin Airport carried out the passenger elevator according to the actual demand every day. Considering that in the actual operation process, the differential pressure and temperature sensor signals fluctuate due to the influence of vehicle running bumps and sensor sensitivity, data cleaning and smoothing are performed in the processing of remote monitoring data. Figure 6 shows the average daily operation time, accumulated operation time, and DPF pressure drop characteristics of the passenger elevator vehicle in actual operation.

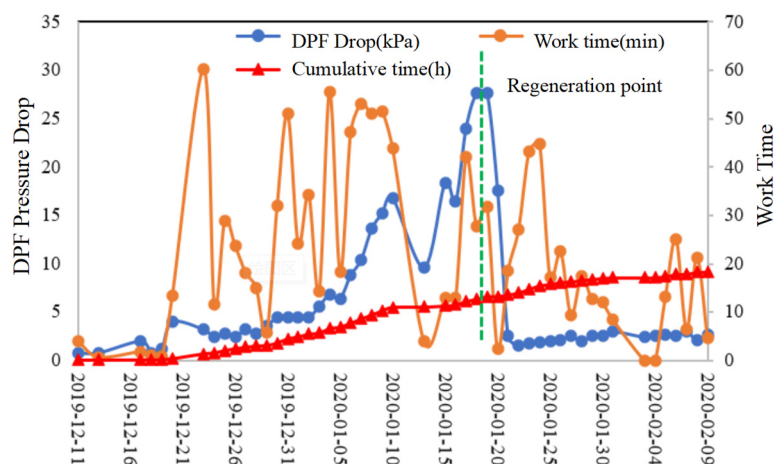


Fig.5 Characteristics of average daily operating time, cumulative operating time, and DPF pressure drop

It can be seen from Figure 5 that the average daily operation time of the passenger elevator vehicle in actual operation is in the range of 15-50 minutes for a long time. The main reason is that the increase in the exhaust volume of the passenger elevator during long-term operation leads to an increase in the carbon load in the DPF, but the exhaust temperature is low and it is difficult to carry out passive regeneration. The pressure drop of the DPF tested in this paper is about 0.5kPa under fresh conditions. With the daily operation of the passenger elevator, the pressure drop of the DPF gradually increases. After the DPF pressure drop reaches the regeneration warning limit of 28kPa, the DPF needs to be regenerated by offline electric heating. After regeneration, the DPF pressure drop of the passenger elevator car is reduced to 2.5kPa in daily operation, which is an increase of 1.7kPa compared with 0.8kPa in the fresh state. Among the particles captured in the main DPF, the particulate matter components such as ash and sulfate cannot be regenerated, therefore, remain inside the DPF increasing pressure drop.

To study the passive regeneration process of the DPF during the operation of the passenger elevator car, the author selected a section of DPF inlet temperature and pressure drop data after the passenger elevator car started to run for analysis, as shown in Figure 6.

It can be seen from Figure 6 that the DPF inlet temperature gradually increases from the ambient temperature of 0°C after the passenger elevator car is started, and the DPF pressure drop is 6.8kPa at this time. After the passenger elevator car runs for 40 minutes, the inlet temperature of the DPF reaches 300 °C, and the DPF starts passive regeneration, but the DPF pressure drop still fluctuates and rises. The rate is higher than the regeneration rate. When the exhaust gas temperature reaches 420°C, the regeneration rate of DPF is higher than the capture rate, and the pressure drop starts to decrease rapidly from 25kPa. After about 10min of operation, the pressure drop drops to 9kPa. At this time, the inlet temperature and pressure drop of DPF do not change significantly.

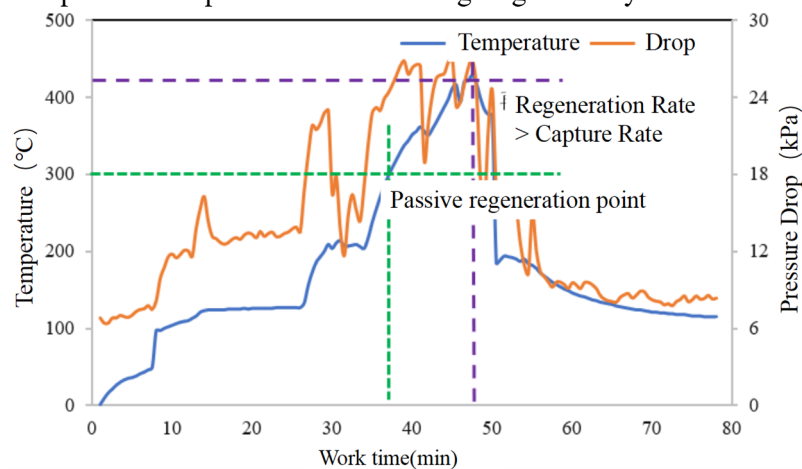


Fig.6 Changes of inlet temperature and pressure drop during DPF passive regeneration

4.3. Influence of vehicle hot and cold start state on DPF emission reduction performance

To study the influence of DPF on the mass and concentration emission characteristics of particulate matter with different particle sizes under the two states of cold start and hot start of the vehicle, this paper selects the DPF after offline regeneration to carry out the particle filtration efficiency test under actual road operating conditions. To sum up, it can be seen that the quality of diesel vehicle particles is mainly concentrated on large particles. With the increase of particle size, the quality becomes larger and larger. In contrast, the quantity is mainly concentrated on small particles, and the peaks are mainly concentrated at 0.02 μ m and 0.12 μ m.

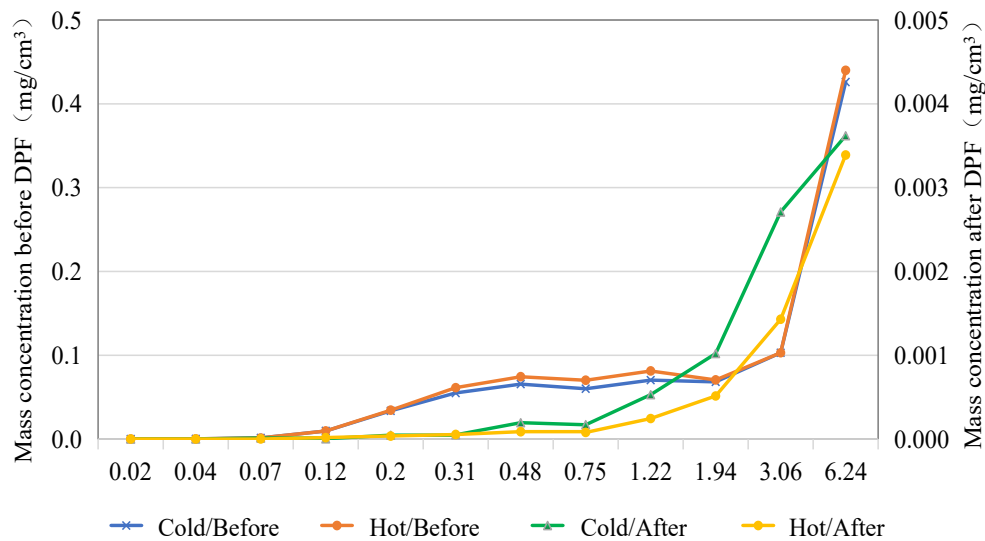


Fig.7 Changes of particle mass concentration before and after DPF under different start-up states

It can be seen from Figure 7 that the mass concentration emission of particulate matter in the two states of cold and hot start is mainly concentrated on large particles with a particle size greater than 3.06 μm , and the mass concentration of the DPF front end is the same in the two states, which also indicates that the hot and cold start had no effect on the mass emission of particulate matter from the test vehicle. However, for the mass concentration of particulate matter at the back end of the DPF, the mass concentration at the back end of the DPF in the cold start state is significantly higher than that in the hot start state. The main reason is that the temperature at the inlet end of the DPF and in the carrier is slow in the cold start state, failing the DPF to regenerate the particulate matter. When starting, the residual particles at the outlet end will be blown out, resulting in a high concentration of particulate matter.

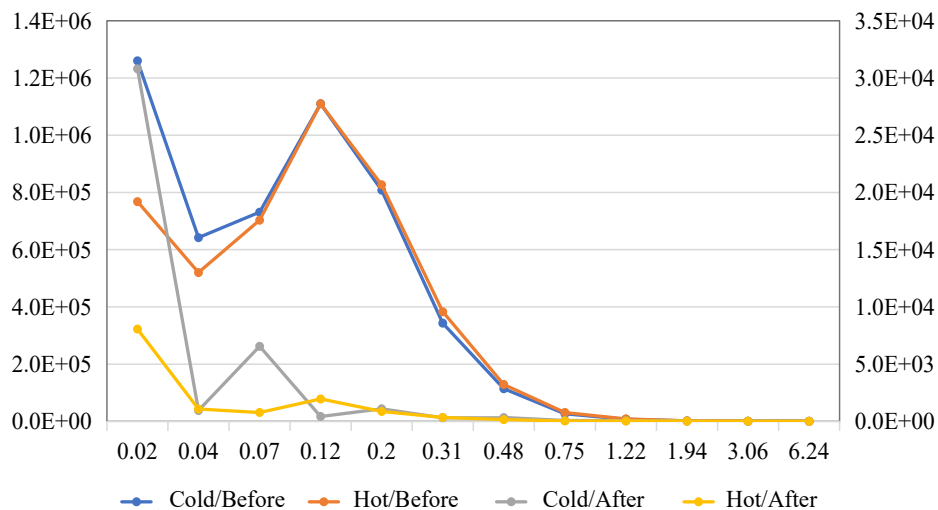


Fig.8 The quantity concentration of particulate matter in front of DPF

It can be seen from Figure 8 that the distribution trend of the number concentration of particles before and after DPF with the particle size is completely consistent. The number of particles is mainly concentrated in the small particle size, and the number concentration of particles shows two peaks with the particle size distribution, which are particles with a particle size of 0.02 μm and a particle size of 0.12 μm . As the particle size increases, the number of particles emitted becomes less and less. When the particle size is greater than 0.75 μm , the number concentration of particles changes very little,

which is several orders of magnitude different from the peak value of the wave.

It can be seen from Figure 8 that the mass concentration emission of particulate matter in the two states of cold and hot start is mainly concentrated on large particles with a particle size greater than $3.06\ \mu\text{m}$, and the mass concentration of the DPF front end is the same in the two states, which also indicates that the hot and cold start had no effect on the mass emission of particulate matter from the test vehicle. However, for the mass concentration of particulate matter at the back end of the DPF, the mass concentration at the back end of the DPF in the cold start state is significantly higher than that in the hot start state. The main reason is that the temperature at the inlet end of the DPF and in the carrier is slow in the cold start state, failing the DPF to regenerate the particulate matter. When starting, the residual particles at the outlet end will be blown out, resulting in a high concentration of particulate matter.

5. Conclusion

(1) The DPF pressure drop prediction model was introduced to calculate the theoretical pressure drop to correct the unreasonable data generated by special working conditions. The time gradually increased, and the regeneration limit was reached after 13 hours of cumulative operation; after offline electric heating regeneration, the pressure drop increased by 1.7kPa compared with the fresh state due to the existence of ash.

(2) When the inlet temperature reaches 300°C , the DPF starts passive regeneration. At this time, the regeneration amount is lower than the deposition amount, and the pressure drop still increases. When the exhaust temperature reaches 420°C , the DPF regeneration rate is higher than the capture rate, and the pressure drop starts rapidly from 25kPa, decreases, and stabilizes after dropping to 9kPa.

(3) The mass distribution of diesel particulate matter is mainly concentrated on large particles, while the number is mainly concentrated on small particles of $0.48\ \mu\text{m}$, of which $0.02\ \mu\text{m}$ and $0.12\ \mu\text{m}$ particles have the largest number. The number of particles with a particle size larger than $0.75\ \mu\text{m}$ is smaller than the peak number of single particle size in the order of magnitude.

(4) After offline electric heating regeneration, the filtration efficiency of DPF for PM and PN is greater than 97% under cold start and hot start conditions. Overall, the efficiency is higher under hot start conditions, but the fine particles and filtration efficiency of particles with a particle size of $3.06\ \mu\text{m}$ are poor; for fine particles with a diameter of less than $0.12\ \mu\text{m}$ and larger particles with a particle size of greater than $0.75\ \mu\text{m}$, the filtration efficiency of the vehicle at cold start is significantly smaller than the hot start.

References

- [1] Orihuela M P, Gómez-Martín A, Miceli P, et al. Experimental measurement of the filtration efficiency and pressure drop of wall-flow diesel particulate filters (DPF) made of biomorphic Silicon Carbide using laboratory generated particles. *Applied Thermal Engineering*, 2018, 131: 41-53.
- [2] A S M, B P S. Particulate matter formation and its control methodologies for diesel engine: A comprehensive review[J]. *Renewable and Sustainable Energy Reviews*, 2017, 80:1227-1238.
- [3] Torregrosa, Antonio José, Serrano, José Ramón, Piqueras P, et al. Experimental and computational approach to the transient behavior of wall-flow diesel particulate filters[J]. *Energy*, 2017, 119:887-900.
- [4] Three-Year Action Plan for Winning the Blue Sky Defense War (7) [J]. *Energy and Conservation*, 2019(05):1.
- [5] ROSSOMANDO B, ARSIE I, MELONI E, et al. Experimental test on the feasibility of passive regeneration in a catalytic DPF at the exhaust of a light-duty diesel engine, F, 2019 [C]. SAE International.
- [6] CHEN C, YAO A, YAO C, et al. Experimental study of the active and passive regeneration procedures of a diesel particulate filter in a diesel methanol dual fuel engine [J]. *Fuel*, 2020, 264.

- [7]PU X, CAI Y, SHI Y, et al. Diesel particulate filter (DPF) regeneration using non-thermal plasma induced by dielectric barrier discharge [J]. Journal of the Energy Institute, 2018, 91(5): 655-67.
- [8]Ban Zhibo, Zhang Yang, Huang Haozhong, et al. Experimental Research on DPF Passive Regeneration Characteristics of Large Diesel Engines[J]. The foreign internal combustion engine, 2017(1).
- [9]Yuan Shouli, Du Chuanjin, Yan Fuwu. Research on DPF Regeneration Technology of Diesel Engine Based on Additive and Electric Heating [J]. Vehicle Engine, 2007, 000(3): 75-8.
- [10]CHIAVOLA O, CHIATTI G, CAVALLLO D M, et al. Modeling of Soot Deposition and Active Regeneration in Wall-flow DPF and Experimental Validation; proceedings of the SAE 2020 International Powertrains, Fuels and Lubricants Meeting, PFL 2020, September 22, 2020 - September 24, 2020, Virtual, Online, Poland, F, 2020 [C]. SAE International.
- [11]Konstandopoulos, A.G., Kostoglou, M., Skaperdas, E., Papaioannou, E. et al., "Fundamental Studies of Diesel Particulate Filters: Transient Loading, Regeneration, and Aging," SAE Technical Paper 2000-01-101625, 2000.
- [12]Li Zhijun, Huang Qunjin, Wang Nan, et al. Pressure Drop Characteristics and Influencing Factors of Diesel Engine DPF Asymmetric Orifice[J]. Journal of Internal Combustion Engines, 2016, 034(002): 135-141.
- [13]CHARBONNEL S, OPRIS C N. Fundamental diesel particulate filter (DPF) pressure drop model, F, 2009 [C]. SAE International.
- [14]Sumit B, Matthew H, Pushkar T, et al. Filtration Efficiency and Pressure Drop Performance of Ceramic Partial Wall Flow Diesel Particulate Filters[J]. Sae International Journal of Fuels & Lubricants, 2013, 6(3): 877-893.
- [15]ZHAO C, ZHU Y, HUANG S. Pressure Drop and Soot Accumulation Characteristics through Diesel Particulate Filters Considering Various Soot, and Ash Distribution Types [J]. 2017, 1.
- [16]PENGHAO J, ZHIJUN L, QIANG L, et al. Simulation of low-temperature combustion mechanism of different combustion-supporting agents in close-coupled DOC and DPF system [J]. ISA Transactions, 2018, 78(88-97).
- [17]Zhang Wei, Shi Weibin. Research on GPSR Routing Protocol for Wireless Sensor Networks[J]. Electronic measurement technology, 2010, 000(009):118-121.
- [18]Marjamki M, Jorma Keskinen §, Chen D R, et al. PERFORMANCE EVALUATION OF THE ELECTRICAL LOW-PRESSURE IMPACTOR (ELPI)[J]. Journal of Aerosol Science, 2000, 31(2): 249-261.
- [19]LIN Z, HUANG Y, XIE Y-J, et al. Remote Monitoring System of Track Cleaning Vehicles Based on 4G-Network; proceedings of the 2020 IEEE International Conference on Networking, Sensing and Control, ICNSC 2020, October 30, 2020 - November 2, 2020, Nanjing, China, F, 2020 [C]. Institute of Electrical and Electronics Engineers Inc.
- [20]KARAMITROS D, AVGERINOS C, SKARLIS S, et al. Model-based comparison of passive SCR after-treatment systems for electrified diesel applications; proceedings of the SAE 3rd CO2 Reduction for Transportation Systems Conference, CO2 2020, July 7, 2020 - July 9, 2020, Turin, Italy, F, 2020 [C]. SAE International.